The Trapping of Agulhas Rings in the South Brazil Bight

Piero S. Bernardo[1], Cauê Z. Lazaneo[1,3], Ilson C.A. da Silveira[1], João P. M. Amorim[1], Milton Borges-Silva[1], Pedro W. M. Souza-Neto[1], Marcelo Dottori[1], Wellington C. Belo[2], Renato P. Martins[2], Luiz A. A. Guerra[2], Daniel L. Moreira [2]

[1]Oceanographic Institute of the University of São Paulo, São Paulo, Brazil
[2]Centro de Pesquisas, Desenvolvimento e Inovação Leopoldo Américo Miguez de Mello of PETROBRAS, Rio de Janeiro, Brazil
[3]Department of Environmental Earth System Science, Stanford University, Stanford, California

Key Points:

- Surrounding cyclonic eddies compresses the Agulhas Rings over the São Paulo Plateau, trapping them in the Brazil Current domain.
- About 95% of the remote anticyclones observed in the South Brazil Bight are considered Agulhas Rings impinging towards the Brazil Current.
- The Agulhas Rings becomes quasi-steady at the South Brazil Bight, occupying a plateau for more than 2/3 of the year.

Corresponding author: Piero S. Bernardo, piero.bernardo@usp.br

Abstract

The South Brazil Bight is a section of the Brazilian margin mainly dominated by the poleward Brazil Current flow, their meanderings and eddies. We evaluated the mean mesoscale for the region, and an anticyclonic feature was highlighted over the São Paulo Plateau. Around that feature, cyclonic eddies were also accentuated. The combination of these structures dominate the region, forming an eddy corridor. Using eddy detection dataset, we reveal that the signal on the plateau was directly related to the presence of anticyclones. The cyclones in the region present both local and remote origins, however, most of the anticyclones are from remote sources. More than 95% of these anticyclones were Agulhas Rings, which could or could not have been subjected to splitting or merging processes. On the plateau we observe an average of 5.3 anticyclones per year. However, these rate is related not only to the number of anticyclones but also to the time they remain there. We observe that Agulhas Rings reside in the region for 50.8 days, consequently, they occupy the plateau for almost 75% of the year. During half of the residence time, there is a multi-pattern interaction with cyclones. This relationship between eddies of opposite polarity creates a shielding process. The anticyclones become shielded and trapped by the cyclones, have their progress delayed, and their course deflected toward the Brazil Current. This was the first observation of this process involving the Agulhas Rings and the first study of the subsequent eddy-current interaction in the region.

Plain Language Summary

The South Brazil Bight is a section of the Brazilian coastline where the ocean current flows mainly towards the south, causing meandering and swirling movements in the water known as eddies. We evaluated the patterns of these activities and found a specific anticlockwise swirling signature over the São Paulo Plateau that is surrounded by clockwise features. We discovered that the presence of anticyclones (eddies that spin in the contourclockwise direction) was directly related to this signature on the plateau. Most of these anticyclones were found to come from a distant source called the Agulhas Retroflection, therefore being called Agulhas Rings. We observed an average of 5.3 anticyclones per year in the area, but it's not just the number that matters - it's also how long they stay there. We found that the Agulhas Rings can stay in the region around 2/3 of the year. During that time, they can interact with cyclonic eddies (spin in the clockwise direction) in a way that slows them down and redirects their course towards the Brazil Current. This was the first time this process was observed in this region, and it sheds light on how these eddies and currents interact with each other.

1 Introduction

The Brazilian Southeast continental margin is characterized in the southernmost portion by the presence of the South Brazil Bight (SBB, 23° S–28.5° S) (Zembruscki, 1979; Castro & Miranda, 1998; Campos et al., 2000). The Brazil Current (BC) flows poleward adjacent to the shelf break along the margin. Due to the shelf break geometry and the vertical structure of the BC, unstable meanders and eddies are formed along the bights (Schmid et al., 1995; Silveira et al., 2004; Calado et al., 2006; Silveira et al., 2008; Uchoa et al., 2022). Underneath the BC, the Intermediate Western Boundary Current (IWBC) flows in the opposite direction (Böebel et al., 1999; Silveira et al., 2000, 2004). This reverse flow enhances vertical shear and energy dissipation at the pycnocline level (Lazaneo et al., 2020) and triggers eddy formation (Mano et al., 2009; Napolitano et al., 2021). This configuration is the source of available potential energy that fuels baroclinic instability and makes cyclonic eddies grow (Silveira et al., 2008; Calado et al., 2008; Rocha et al., 2014). It has been reported that these cyclones only translate to either north or south after being pinched off from the BC (Arruda et al., 2013; Mill et al., 2015; Pereira et al., 2019; Silveira et al., 2023). However, BC-IWBC instability might not be the only

mechanism influencing the formation and propagation source of these cyclones since external sources are plausible.

Among the distinct sources of the vortical features that propagate in the ocean and reach the southeast continental margin of Brazil, remote sources have gained greater focus in the literature. Among these sources, Agulhas Rings (AgRs) have been reported to cross the South Atlantic (Olson & Evans, 1986; de Ruijter et al., 1999; Biastoch et al., 2009), reach the Brazilian SE continental margin, and eventually interact with the BC and its meanders (Guerra et al., 2018; Laxenaire et al., 2018). Guerra et al. (2018) followed one of these AgRs from its origin site to the region off Cape Frio (23° S), where it interacted with two cyclonic eddies (potentially Cape Frio Eddies - CFEs), creating a vortical triplet that propagated southwestward. This cape is a geomorphological feature around which recurrent cyclonic meanders can be formed due to a change in the shelf break orientation. Previous studies have noted that the SBB is a region within the BC domain prone to this kind of oceanic interaction (Assireu et al., 2003; Oliveira et al., 2009).

The arrival of AgRs in the SBB must be frequently considered a relevant trigger for BC instabilities since CFEs and the Cape São Tomé Eddy are formed at a rate of 2.3 eddies per year (Silveira et al., 2023). Using altimeter data and an eddy detecting algorithm, Guerra et al. (2018) estimated that 6 AgRs are formed at the Agulhas Retroflection (AR) on average per year, but only slightly over 50% of them manage to surpass the Walvis Ridge and cross the South Atlantic. Laxenaire et al. (2018) used a more complex eddy-detecting method, identifying 3.5 AgRs, on average, that cross the South Atlantic per year upon analyzing a 24 year long time series. Moreover, these latter authors mentioned that ring trajectories are complex and subject to a series of nonlinear processes, such as splitting and merging.

The translation of the AgR into and through the South Atlantic Ocean is a key component of global ocean circulation (Gordon et al., 1992), connecting the South Atlantic and Indian Ocean gyres (de Ruijter et al., 1999). Due to this, saltier and warmer waters are introduced into the South Atlantic (Lutjeharms & Van Ballegooyen, 1988; Lutjeharms & Cooper, 1996; Biastoch et al., 2009; Nencioli et al., 2018; Capuano et al., 2018; Laxenaire et al., 2020), which makes a significant contribution to the amount of energy available in the Atlantic system (Olson & Evans, 1986). In addition, the Agulhas Leakage has a relevant feedback relationship with the climate system. On the one hand, the number of rings shed between basins is influenced by the position of the westerlies and changes in the wind forcing (Biastoch et al., 2009). On the other hand, the increase in leakage in a warming scenario could affect the Atlantic overturning circulation (Beal et al., 2011) due to the impacts on the global meridional heat flux (Lutjeharms & Gordon, 1987). Although the excess heat gained through the surface can quickly dissipate into the atmosphere (Lutjeharms & Cooper, 1996), the temperature signal can be preserved along the South Atlantic crossing in cases where the rings present a thick thermostat (Souza et al., 2014; Guerra et al., 2018). The AgRs are emitted and move across the South Atlantic in different latitudinal ranges (Laxenaire et al., 2018), crossing the deepest portion of the Walvis Ridge (Schouten et al., 2000)).

Despite these recent findings on how the AgR belt is migrating toward the western side of the South Atlantic, there is still little information about the passage and persistence of these eddies along the SBB and their interactions with the BC. To this end, we begin this article by describing the occurrence of eddies within the limits of the SBB, which are closely related to mesoscale activity. Additionally, we show the arrival of these AgRs in the BC system, their persistence, and possible interactions with oceanic surrounding features, such as cyclones and BC. These interactions are evaluated to better understand their importance and impact on the passage of anticyclones in the region. With this description, we assess how the SBB is dominated by mesoscale vortices over time and how remote structures participate in shaping this hydrodynamic system.

2 Datasets

To explore ocean surface signals linked to mesoscale activities, we employed the multisatellite altimetry Absolute Dynamic Topography (ADT) Level 4 product and derived geostrophic currents produced by the Sea Level Thematic Center (SL-TAC) and distributed by the Copernicus Marine Environment Monitoring Service (CMEMS, `https://www.copernicus.eu/en`) (Pujol & Mertz, 2019). This dataset is gridded at a 1/4°resolution and spans from 1993 to the present. However, this time series is reduced to match the temporal coverage of the other dataset used (Laxenaire et al., 2018).

The altimeter-based eddy-identification algorithm output, developed by Laxenaire et al. (2018, 2020), called "Tracked Ocean Eddies" (TOEddies), was employed. This dataset contains eddy contours that were defined according to the maximum velocity contour around a possible eddy center. Furthermore, this dataset considers the nonlinear interactions of splitting-merging processes and neutral interactions to track cyclonic and anticyclonic eddies in the South Atlantic and in part of the Indian Ocean from January 1, 1993, to May 15, 2017. From this set, we used the daily eddy identification data, which contains, among other variables, eddy contours associated with the eddy maximum speed, the position of the eddy center, the radius, and a tracking index of each eddy over time.

For the eddies shed in the Agulhas Retroflection, Laxenaire et al. (2018) generated a chain of eddies and routes that called the Agulhas Ring Eddy Network (AREN), which connects the South Atlantic to the Indian western boundary. The eddies in this network are classified by order from 0 to 29. The zeroth-order eddies are those whose trajectory originates directly from the Agulhas retroflection region. These routes are referred to as "main trajectories". The other orders represent secondary trajectories connected to the main pathways through splitting and merging events. The eddy orders allows us to assess whether the eddies present in the South Atlantic western boundary have a remote origin, possibly linked to Agulhas Retroflection, or not, as well as their fate. A zero-order eddy that is observed in the western portion of the South Atlantic is a feature that directly crossed the South Atlantic from the Agulhas retroflection region without having constructive or destructive interactions (e.g. (Guerra et al., 2018)).

3 Climatological Stream Function Pattern in the South Brazil Bight

The Brazil Current is shallow and weak compared to its analogs in other ocean basins (Silveira et al., 2000), with its core approximately positioned over the 1000 m isobath (Rocha et al., 2014). Therefore, this isobath becomes an important reference for local mesoscale dynamics. In local terms, this mesoscale activity is directly related to the shoreline orientation south of 23° S and to BC meandering, as seen in other cases, such as cyclone formation at Vitória-Trindade Ridge (Schmid et al., 1995; Uchoa et al., 2022), Cape São Tomé and Cape Frio (Calado et al., 2010; Palóczy et al., 2014; Silveira et al., 2023). In addition, remote eddies reach the SBB and interact with BC mesoscale features (Guerra et al., 2018).

We first compute and discuss the mean pattern of the circulation in the SBB to seek a meandering BC pattern and other structures that may indicate recurrent and/or permanent mesoscale vortical features. We opted to build mean stream function fields from the ADT daily maps by simply using

$$\Psi = (\frac{g}{f_0}) \times \mathrm{ADT}\ , \tag{1}$$

where f_0 is the Coriolis parameter evaluated at the central latitude of the SBB. We then normalize the Ψ maps by subtracting the mean value and dividing by the standard deviation related to that average. Over the normalized maps, we calculated the 1993–2017 average Ψ map (Figure 1.A). Our intent with normalization is to highlight the Ψ-lines

associated with features of different polarities (Figure 1.A). Hereafter, we refer to these averaged and normalized values as Ψ only.

We depict a concentration of the most negative Ψ values (between -0.4 and -0.6$\times 10^4\,m^2\,s^{-1}$) in a zone along the 1000 m isobath from 23° S to 31° S, as shown in Figure 1.A. On the shallower side, there is a band with positive Ψ values closer to the shelf break. The positive side of this bipolar pathway is mostly related to BC. Intrinsic to the current axis signal, we observe the effect of recurrent cyclonic meandering. The signature of recurrent CFE formation at 25° S, as well as the Cape Santa Marta Eddy (29° S), is clear. The negative side of the bipolar pathway is associated with the recurrent anticyclonic activity (Figure 2.A). This anticyclonic pattern, in addition to the meandering cyclonic aspect of the BC, creates an "eddy corridor" at the SBB, as originally suggested by Belo (2011), and is analogous to what was defined by Garzoli and Gordon (1996) for the Benguela Current.

To better identify sites of permanent and/or recurrent mesoscale phenomena, we eliminate the underlying large-scale background by applying a 181-day Blackman high-pass filter in each grid point of the time series. This filter application reduced seasonal variability and allowed us to calculate a long-term "mesoscale mean field" (Figure 1.B). The long-term mesoscale mean field depicts the dominance of some distinct patterns. The first prominent feature is a negative closed contour centralized at 26.5° S–43.5° W over the São Paulo Plateau (SPP, the 2500 m isobath is used as a reference for this feature). This structure indicates the recurring sign of an anticyclone. Southwest of this contour, a continuous anticyclonic strip appears to be confined between the 1000 m and 2500 m isobaths. In the eastern portion, another negative closed contour is present at 26° S–40.5° W.

After the filtering process, the SBB's recurrent cyclonic features are also highlighted (Figure 1.B). We emphasize that there are indications of recurrent cyclonic structures outside the BC domain in the map. Centered at 28° S–44.5° W, there is a positive (cyclonic) closed contour and another vortical feature with lower Ψ values at 27.5° S–41.5° W. The presence of a recurrent cyclone oceanward of the BC domain is not observed in the unfiltered mean field, where negative values are mainly depicted in the same region (Figure 1.A). This recurrent aggregation of cyclonic structures seems to confine the recurrent anticyclonic signal. This potential containment appears to restrict the anticyclonic pathway and compresses it against the BC. To the northwest (25.5° S–44.5° W) and northeast (24.5° S–42.5° W) of this main negative recurrent feature, we observe recurrent cyclonic meanders and eddies from the BC (Calado et al., 2006, 2008; Uchoa et al., 2022), which are close to and/or greater than zero, confining the anticyclonic structure.

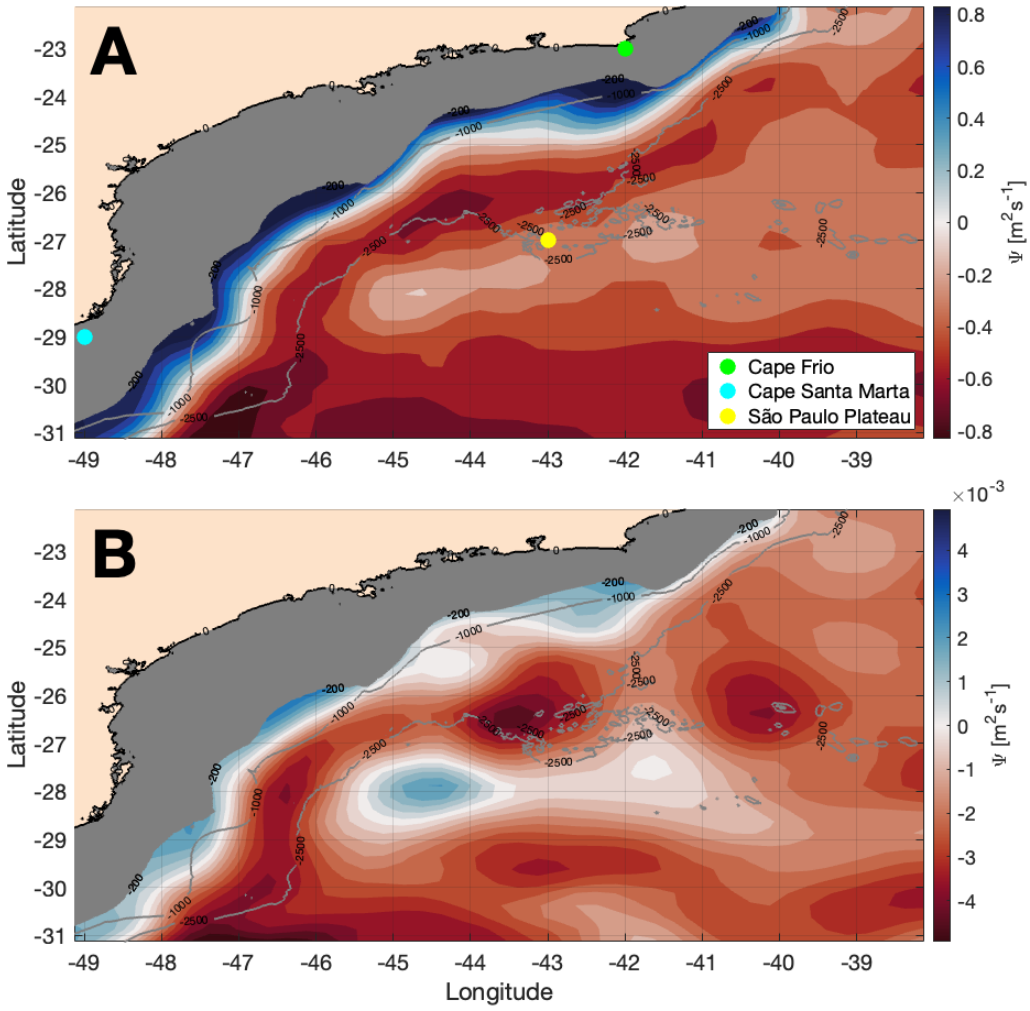

Figure 1. A. Normalized mean field and B. filtered mean field (181-day high-pass Blackman filter by convolution) of the stream function field (Ψ) for the South Brazil Bight between January 1993 and May 2017. Negative values are related to anticyclonic features, and positive values are related to cyclonic features. The grey mask extends from the coast down to the 200 meter isobath, and the 1000 and 2500 meters isobaths are indicated.

4 Climatological Eddy Occurrence Rates

The climatological Ψ maps (Figure 1) exhibited various vortical features although the whole time series (1993–2017) was used to develop them. The series length is still not long enough to smooth the eddy signals from the mean circulation maps. The eddies are so evident that we discuss them almost as synoptic features in the following section. Certainly, from the works by Guerra et al. (2018) and Laxenaire et al. (2018), we know that these vortical features are recurrent, remote-origin anticyclones and cyclones that arrive continuously in the SBB. The sites where these "mean eddies" are depicted are probably subjected to higher occurrence rates and more frequent pathways.

To identify whether the patterns observed in the mesoscale mean field are related to the eddy occurrences, we start by picking the daily eddy contours associated with the

eddy maximum speed within the SBB using the Laxenaire et al. (2018) identification set. Then, we map the points in the interior of the eddy contours for each day of the time series. From these daily SBB eddy maps, we estimate the occurrence rate of cyclones and anticyclones per grid point (0.05°×0.05°grid) and create a 2D histogram (Figure 2).

Based on these occurrence rate maps, we can confirm the direct relationship between the above mentioned average maps (Section 3) and the presence of eddies with opposite polarities in the region. This assessment corroborates the vast presence of vortices in the region also found by Rocha and Simoes-Sousa (2022). Analyzing the anticyclonic cases (Figure 2.A) shows that anticyclonic eddies occur with the highest frequency ($\geq$25%) near the 2500 m isobath and is confined to the 1000 m isobath to the north, reinforcing the eddy corridor configuration mentioned before. In addition, most anticyclones ($\sim$40%) occur over the São Paulo Plateau (Figure 2.A), coinciding with the closed contour of minimum Ψ values (Figure 1.B). This higher occurrence rate stands out because the eddy corridor already presents recurrent structures, and there is an even greater persistence or concentration of anticyclones in this specific site.

As previously observed in the mesoscale mean field (Figure 1.B), the anticyclonic structure over the SPP is commonly surrounded by cyclonic features. This belt-shaped cyclonic feature that surrounds the persistent anticyclonic region (red line in Figure 2.B), although not necessarily occurring simultaneously, suggests the capacity to confine these anticyclones. Moreover, the cell centered at 28° S–45° W, with an occurrence rate near 25%, matches the positive sign in Figure 1.B, which is southwest of the anticyclonic feature. Cyclonic occurrence is also notable on the continental slope, centered at 24.5° S–42.5° W (Figure 1.B). This outstanding formation is due to the recurrence of the CFE, which is directly related to the BC meander and plays an important role in the formation of dipoles with AgRs that arrive in the western portion of the South Atlantic, such as the one observed by Guerra et al. (2018).

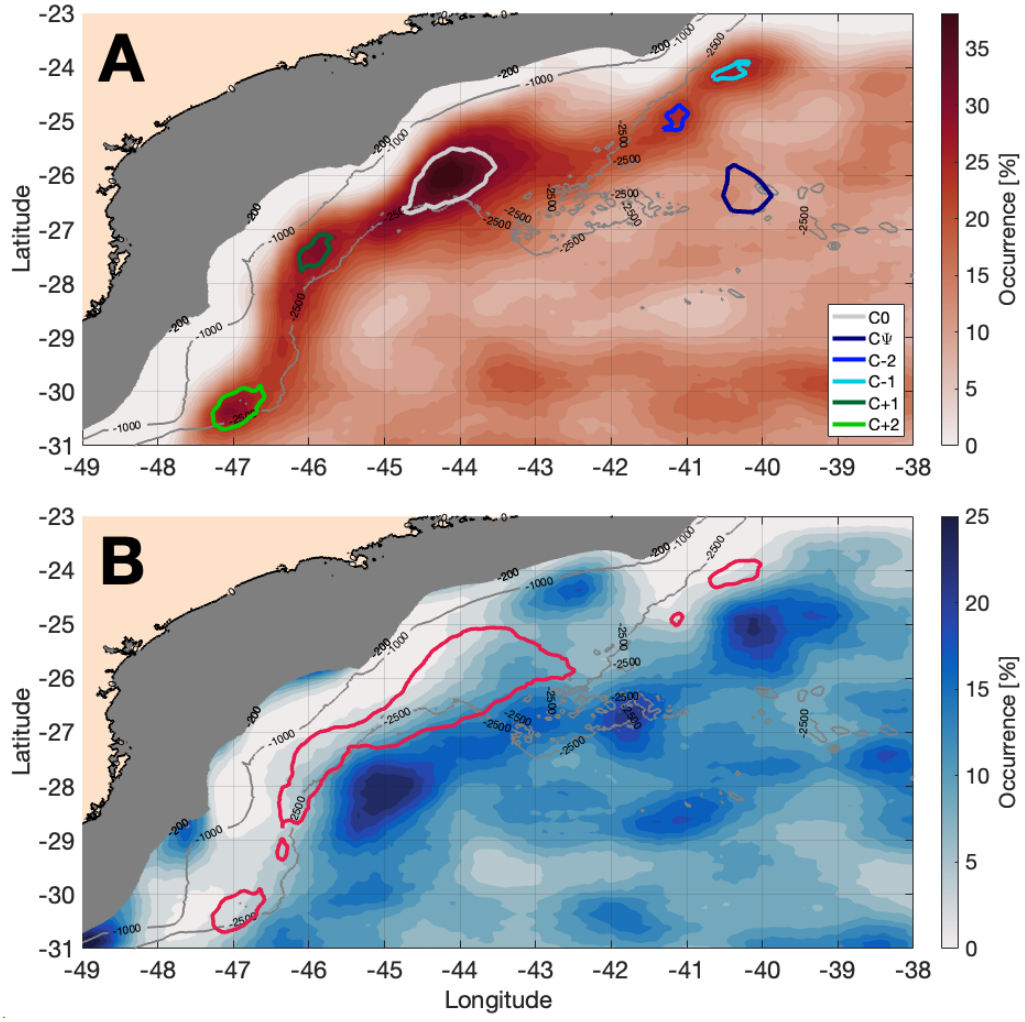

Figure 2. Occurrence of A. anticyclonic and B. cyclonic eddies in the South Brazil Bight between January 1993 and May 2017, according to the identification data from Laxenaire et al. (2018). The closed contours in panel A represent the center of the rings' path (C0) within the SBB; the two secondary occurrence maxima northeastward (C-2 and C-1) and southwestward (C+1 and C+2) related to C0; and the contour related to the structure centered at 26° S–40.5° W in Figure 1.B (CΨ). The red contour in panel B indicates the isoline of the 25% anticyclonic occurrence. The gray mask extends from the coast down to the 200 meter isobath, and the 1000 and 2500 meters isobaths are depicted.

5 Anticyclone origin, trajectory and fate

Initially, the focus is directed on the anticyclonic features, as these are the most outstanding mesoscale features in the region (Figure 1.B) and are still not well documented. It is possible to identify subregions of higher occurrence based on the map of Figure 2.A. These maps reveal the spatial and temporal distribution of the anticyclones that cross the SBB. Aiming to sectorize the SBB to better understand the passage of anticyclones in the basin, we defined contours over localities with high occurrence ($\geq$25%) as a reference for the upcoming analyses. The area with the highest occurrence rate over the

SPP is qualified as the center of the rings' path (C0) within the SBB. We assume that the anticyclones may converge in that location.

We selected two secondary maxima of occurrence northeastward (C-2 and C-1) and southwestward (C+1 and C+2) of the central passage area C0. We define these contours to investigate the paths that the anticyclones take before and after reaching C0. There is a convergence of anticyclonic occurrence in the C-2 and C-1 regions. There is a tendency for eddies to move by self-induced propulsion (Cushman-Roisin et al., 1990) or to be transported northwest in the open ocean until they encounter a physical barrier, such as the Brazilian continental slope (Azevedo et al., 2012). Upon reaching the western continental margin, the AgRs, for example, tend to typically transit southwest, arriving south of Cape Frio (Guerra et al., 2018). Therefore, the secondary maxima C+1 and C+2 are the result of these eddies propagating in the same direction as the BC, as shown in Rocha and Simoes-Sousa (2022). Finally, we select another contour, named CΨ, that despite not appearing as an anticyclonic high occurrence region in the Laxenaire et al. (2018) dataset, stands out in Figure 1.B (negative Ψ-values centered at 26.5° S–40.5° W).

The anticyclone occurrence contours, used as checkpoints, allow for the eddies to be classified based on different scenarios: (i) eddies formed within the corridor itself by the nonlinear interactions of preexisting features, (ii) the arrival of remote rings, and (iii) based on their transit toward the southwest while already in the SBB. To evaluate these three scenarios, we considered a valid anticyclonic event to be the one that stays within the reference C0 contour for at least one day

From the selected anticyclones, we develop three quantities to indicate how anticyclones occur in each of the reference C contours (Table 1). The residence time (RT) is calculated based on the length of time that the eddy contour remains in the reference area. The yearly residence (YR) is the time per year that each area is occupied by one or more of the selected anticyclones, leading to the estimation of the number of anticyclones per year (AY) at each one of the C contours.

We next explore two elements: the number of anticyclonic eddies (Section 5.1) and the residence time along the SBB (Section 5.2). The combination of these factors shows us if the occurrence rate is related to a high repetition of anticyclonic events or the permanence of these eddies in a specific C area.

5.1 Incidence of rings in SBB

Examining the results for the C0 contour shows that 136 rings were recorded within it between 1993 and May 2017 (Figure 2.A). By applying the AREN classification system, used to determine which anticyclones come from the Agulhas Retroflection (Laxenaire et al., 2018), it was shown that 130 rings were considered as AgRs, categorized in different orders. The remaining 6 did not show remote connections. This demonstrates the influence that rings shed remotely and propagated across the South Atlantic have over the SBB. From now on, we only analyse these 130 AgRs.

This comprehension of the anticyclone origin is important because the Agulhas Retroflection is a unique connection between basins, introducing distinct waters from the Indian Ocean to the South Atlantic Ocean (Gordon, 1986), with the potential to carry the influence from one western boundary current to another (Guerra et al., 2022). If this ring is transported directly from the Agulhas Retroflection, without any nonlinear interactions, the content present in this eddy is potentially better preserved. When interactions occur, the anomaly carried into the SBB can be mitigated (Nencioli et al., 2018; Laxenaire et al., 2020). This shows that it is essential to consider interplays, which are an important part of the lifetime of these eddies. Despite having a similar origin, the rings are dissimilar in how they cross the South Atlantic. Of the 130 AgRs present at SBB,

only 3 cross directly, without undergoing splitting/merging processes (Figure 3.B), which is similar to those investigated by Guerra et al. (2018).

Once we know a given anticyclone origin, we evaluate its arrival at the western South Atlantic basin, as well as its trajectory along the SBB (Figure 3.A). Aside from the three zeroth-order eddies that reach the western portion of the South Atlantic, the remainder had several nonlinear interactions along their path. Their trajectories across the South Atlantic are split into threaded segments until one last interaction gives rise to an anticyclone that enters the SBB system (Figure 3.B). Upon that observation, 53.1% of the AgRs' last segment started before the arrival at the SBB, 36.9% occurred inside the SBB, and 10% do not cross the reference contours. Therefore, the latter are disregarded in our analysis. Of the AgRs that approach the western edge of the South Atlantic, between 24° S and 26° S, 90% do so in three different ways: (i) the anticyclones reach C-2, cross it, and proceed to C-1; (ii) the anticyclones arrive directly in C-1, and (iii) the anticyclones pass through CΨ to enter the bight. It is important to establish that it was not possible to determine if there is a preferred route among the three because, in some cases, the same ring can pass through all three areas.

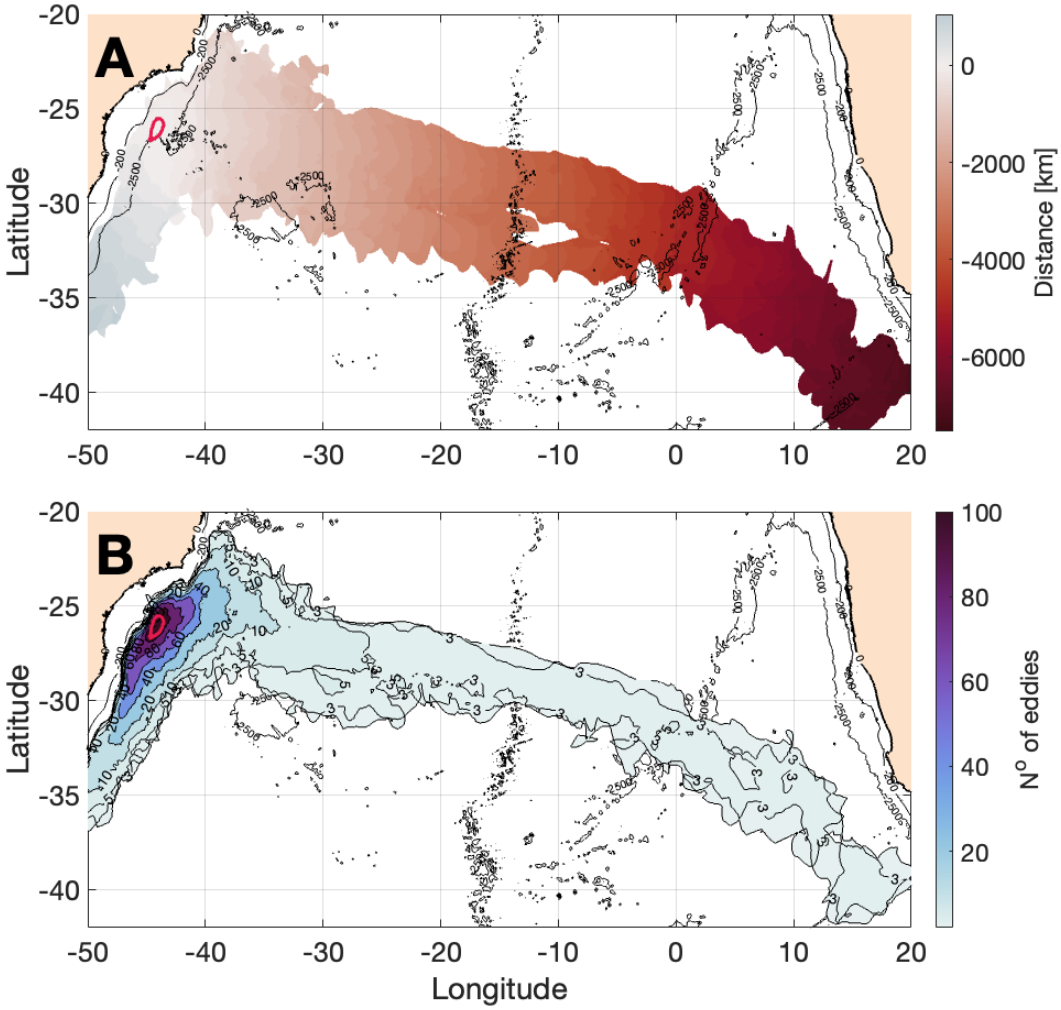

Figure 3. A. Distance covered by the Agulhas Rings (AgRs) before (red) and after (blue) crossing the C0 contour and B. the number of AgR segments that reached and crossed the C0 contour along the South Atlantic between January 1993 and May 2017, according to the identification data from Laxenaire et al. (2018). The 200 meter and 2500 meter isobath is shown in gray, and the C0 contour is shown in magenta.

Table 1 shows that a greater number of AY (5.3±1.3) in C0 than in the northernmost contoured areas (C-1, C-2 and CΨ) since there is a convergence of routes in this region. However, this amount does not represent a sum of the AY in the C-1 and C-2 contours. This can be due to 3 factors: (i) not all AgRs cross C0; (ii) a single event is counted in more than one C contour; and (iii) anticyclonic eddies merged within C0. For (i), out of the 213 rings that pass through the northernmost C contours, ²/₃ do not reach contour C0. However, 47 of these do generate new anticyclones that reach C0 by splitting. For (ii), 109 rings are counted passing through more than one C-contoured area. For item (iii), there are 24 anticyclonic eddies that merge in C0, of which 92% involve mergers to rings that are already in C0. There are also anticyclones that are destroyed in C0, without undergoing any merging processes. Some of these can meld with the BC anticyclonic lobe and are, therefore, absorbed by the current. Other eddy-killing pro-

cesses have been reported by Renault et al. (2019) for the Gulf Stream and Agulhas Current but not for the BC.

Not every anticyclone proceeds to C+1 or even to C+2 after passing through the C0 contour. Only 64.1% and 38.5% of the AgRs reach these contours, respectively. Thus, although the AY quantity is similar or greater, comparing C+1 and C+2 to C0, some of these values are associated with the 144 anticyclones that arrive directly at C+1 or C+2. Knowing that more than 83% of these are AgRs of different orders, there is a clear dominance by remotely originated anticyclonic eddies throughout the entire SBB.

We can therefore infer from our analysis that there are multiple patterns in both how AgR eddies arrive at SBB and how the bight is crossed. In addition, merging and splitting processes may occur within the basin, generating new possibilities for the trajectories and fate of these rings. Thus, evaluations of only the amount of AgRs present in the SBB and their paths does not explain the highest occurrence rates that exist within the C0 contour over the SPP, as seen in Figure 2.A. If that were the case, these rates would be similar between the C0 and C+1 contours and even higher in C+2, the contour where there the passage of anticyclones per year (AY) is highest.

Table 1. The number of anticyclones per year (AY), average residence time (RT) and yearly residence (YR) that cross each contour and belong to Agulhas Rings Eddy Network (AREN); Number of cyclones (NC) that interact with the AgRs and the mean interacting time (IT).

Contours	AY	RT (days)	YR (days)	NC	IT (days)
CΨ	3.3±1.2	35.5±24.7	116.9±46.0	109	12.2±14.9
C-2	4.3±1.6	34.5±25.5	148.4±66.0	112	13.1±15.2
C-1	4.5±1.2	32.3±23.7	147.4±50.3	148	13.9±17.3
C0	5.3±1.3	50.8±31.8	271.2±43.5	219	25.2±22.8
C+1	5.2±1.4	34.5±23.7	178.4±54.9	169	14.6±15.9
C+2	5.8±1.4	29.6±17.9	174.0±37.8	144	10.8±13.9

5.2 SBB Crossing time

In the previous section, we noted that the amount of AgRs that pass through each portion of the SBB does not fully explain the occurrence rates shown in Figure 2.A. In addition, we also note that there is no proportionality between these rates and the number of AgRs in the SBB. This inconclusiveness can be remedied by the time that the anticyclones take to cross each C-countered region. Consequently, it is necessary to study the residence time of the anticyclones in each C region (RT, Table 1).

The C0 contour presents the highest RT. The permanence difference differs by approximately 2 to 3 weeks from the other C-contoured areas. This helps to explain the vortical feature over the SPP shown in Figure 1.B. Additionally, we note in Table 1 that the RTs in the other C contours do not show great variability among themselves, and all are approximately greater than 30 days.

The combination of the annual amount of AgRs (AY) and their permanence (RT) results in an annual occupancy, on average, of almost 75% (YR, Table 1). In addition to the convergence of the arrival pathways, there are also merging events that occur at the C0 site. These factors may contribute to the greater recurrence and permanence of AgRs. Therefore, this shows that the AgRs tend to maintain their integrity longer, without splitting or dissipation. This can also be observed by the fact that the anticyclones in C0 have the highest mean radius values among the contours (121.2 ± 33.8 km). Escudier

et al. (2016) observed that there is a relationship between the duration of eddies and the radial scale in that long-lived eddies tend to reach larger radii more quickly.

The persistence of the rings may be related to conditions intrinsic to the SBB or the rings themselves, such as baroclinic instability (Rocha et al., 2014) or interaction with topography (Soutelino et al., 2013). If the second condition is true, there would be no distinction between the RTs in the different contours. As confirmation, there is no significant correlation between the RT of each eddy and its order or lifetime. The order of each eddy is directly related to the number of nonlinear interactions that these structures went through, according to Laxenaire et al. (2018). The eddy lifetime is related to how long the anticyclone remained nearly intact. The correlation between the travel time of the ring before (-0.03) or after (0.27) passing through C0 and the RT is weak. Therefore, the processes that prolong or shorten the duration of an anticyclone do not appear to influence its persistence in the vicinities of the SPP.

We need to redirect the assessment towards what happens around the anticyclones when they arrive in the SBB, mainly in the C0 region. Figure 1.B shows, as pointed out earlier, that, together with the noticeable anticyclone signature, the surrounding cyclones are also obvious. As seen for the anticyclones, the cyclonic signatures shown in Figure 1.B are directly related to the eddies, which corroborates the high concentration of cyclonic eddy kinetic energy (EKE) observed next to the SPP by Rocha and Simoes-Sousa (2022). In short, in the region where the anticyclonic eddies are permanent, peaks of kinetic energy are observed due to the presence of cyclones around them.

6 The AgR trapping and the role of the cyclones

We now assess the role cyclones play in the stagnation of AgRs over C0. As previously mentioned, other studies have evaluated the formation of cyclones within the basin, which are partially indicated near the shoreline of Figure 2.B. As an example, we observe their climatological signature centered at 24.5° S–42.5° W, closer to the 1000 m isobath (Uchoa et al., 2022). However, little is known about the arrival of cyclones from outside the basin, which reach the study region.

Rocha and Simoes-Sousa (2022), based on EKE maps, observed that the oceanic portion of the SBB is vastly occupied by mesoscale eddies, as seen in Figure 2.B. The authors also noted that local cyclones contribute more to SBB's EKE than remote cyclones. Interestingly, this remote contribution may have greater importance for systems that relies on interactions with anticyclones.

As a hint of the presence of these remote cyclones, Figure 2.B shows a large number of cyclones pairing with the oceanward side of the anticyclonic eddies. The increase in the frequency of the cyclones around the C-2, C-1, C0, C+1, and CΨ areas does not appear to be related to the local formation by the BC (Figure 2.B) but is instead related to eddies that formed remotely. However, despite the observation of this apparent coincident occurrence of anticyclones and cyclones, we cannot confirm that the coincidence occurred simultaneously by only inspecting the aforementioned figure. Thus, the formation of vortical pairs is not guaranteed.

Therefore, to study the co-occurrence of cyclones and anticyclones, we select only anticyclone events that resulted from the Agulhas Retroflection in our analysis. We again only examine the AgRs that cross the C-contoured areas and that remain for more than one day over C0. We identify 117 cases of AgRs that arrived at C0 and occupied it for 6228 days between January 1, 1993, and May 15, 2017, which represent almost 70% of the whole period. We interpret that the interaction of eddies of different polarities occurs when the distance of the eddy cores is shorter than the sum of their radii (Ni et al., 2020). Then, based on the identification of the local and remote cyclones that interact with the anticyclones (Figure 4), we determined the number of cyclones (NC) and the

time of the interaction (IT) (Table 1 and Figure 5.B). We also observe the simultaneous occurrence of cyclones and anticyclones in different C areas, revealing several different patterns of interaction (Figure 6).

Focusing on the interaction events in C0, the AgRs interacted with 219 cyclones over 2947 days (NC, Table 1), without revealing a common established pattern. In most cases (80%), anticyclones interacted with only one cyclone at a time. In the other 20%, interaction with 2 to 4 different cyclones could occur simultaneously. Each anticyclone interacted on average with 1.9±1.3 cyclones during its residence time in C0. As a verification of this result, we show in Figure 5.C that in almost 80% of the cases, the AgRs interacted with 1 to 3 cyclones. For the rest of the cases where interactions occurred (4 to 6 cyclones), we highlight in Figure 5.C how rare it is to observe a single interaction between an AgR and 6 cyclones. Thus, the availability of more cyclones around the anticyclones increases the interaction time (Figure 5.B); however, the configuration pattern is less common (Figure 5).

Another interesting piece of information about these interactive cyclones comes from their remote or local origin. In Figure 4, using the 2500 m isobath as a reference for the SBB limit, we can see that many cyclones come from outside the basin. As AgRs pass through the SBB, they interact with 447 different cyclones, of which 306 originate in regions deeper than 2500 m. Approximately 57% of these 306 cyclones form less than 111 km away from the region where the eddy-eddy interaction is taking place (black line in Figure 4). For the remaining cases (43%, 131) originating outside the SBB, we can see in Figure 4 the beginning of the cyclone track segments coming from either the south or north of the reference contour. Nevertheless, 55% of these originate east of 40° W.

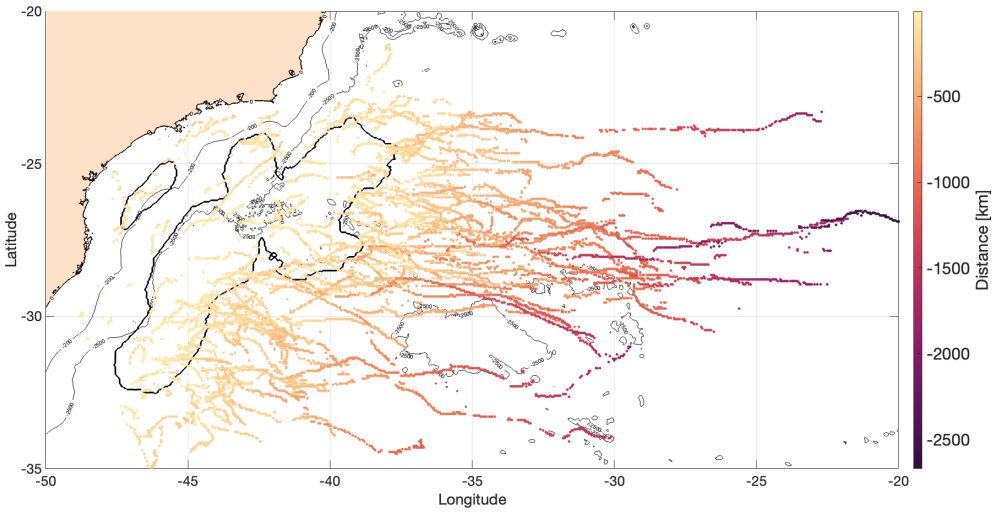

Figure 4. The cyclonic displacement between January 1993 and May 2017 before reaching the position where the interactions occur. The black contour is the region that represents the sum of all cyclone contours in the position when interacting with an AgRs and is used as a reference for the distance estimate. The trajectories are derived from the identification data from Laxenaire et al. (2018), and the points that determine the trajectory represent the center of the moving vortices. The 200 meter and 2500 meter isobath is shown in gray.

This recurring pattern of an anticyclone surrounded by cyclones (Figure 6) has been reported in the literature and is called a "shielded eddy" (Carton, 1992; Reinaud, 2017).

Carton (2001) showed that cyclones survive as localized smaller features surrounding the larger anticyclonic vortical ring by resisting the deformation induced by the interaction. On the other hand, the anticyclone also preserves its integrity and stalls, as seen for the Lofoten basin eddies (Gordeeva et al., 2021). Shielded anticyclones surrounded by smaller-scale cyclones have been observed in the Gulf Stream area (Kennelly et al., 1985), Kuroshio-Oyashio frontal zone (Prants, 2015; Prants et al., 2018), Lofoten Basin (Belonenko et al., 2021) and northwestern Pacific (Prants et al., 2020) during the stagnation phase of anticyclones.

The previous paragraph showed that there is a relationship between the presence of cyclones and the stagnation of anticyclones. In Figure 6, we can observe not only the interaction with the cyclones in the shielding process but also with the Brazil Current (represented by the blue line) on the inshore side of the AgRs. This is the first description of the shielding effect and current-eddy interaction involving AgRs within the SBB. Azevedo et al. (2012) evaluated the encounter between anticyclones and boundary currents and explored how this could impact the current flow and generate a stationary eddy. However, as observed by Guerra et al. (2018), this encounter involves the participation of other vortices, as confirmed in multiple cases in this assessment. These interactions, in addition to impacting the propagation of anticyclones, increase the complexity of encounters between the AgRs and the BC.

There seems to be a direct relationship between the number of cyclones and the residence time in C0 (Figure 5.A). The more cyclones interact with the anticyclone, the longer the stagnation period lasts. However, we observe that the correlation between NC and RT of the 117 anticyclonic events over C0 is only $r = 0.56$. This moderate correlation shows us the importance of the number of cyclones interacting with anticyclones. However, this is not the only factor that impacts stagnation. Both the number of cyclones and the time that these interactions effectively last need to be evaluated.

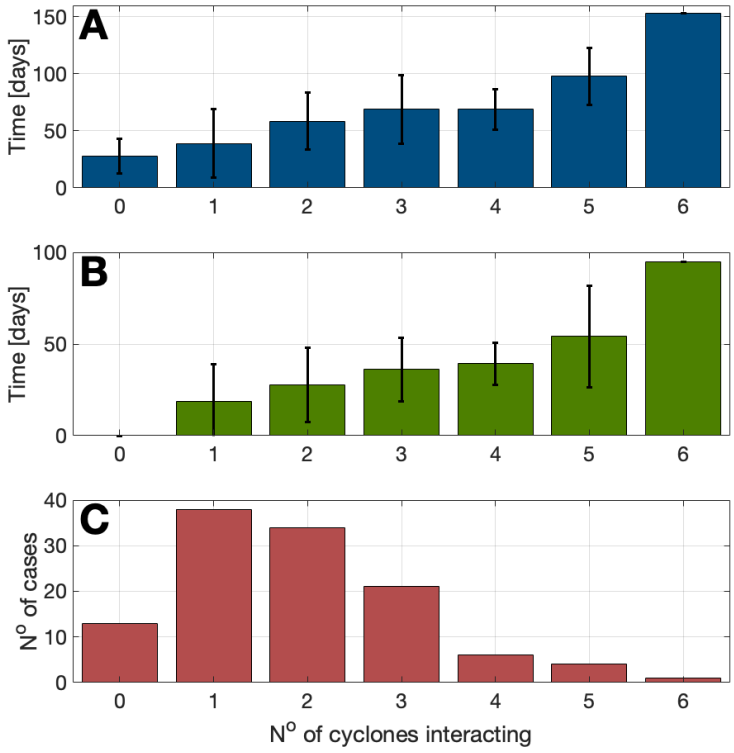

Figure 5. A. Mean anticyclonic residence time in C0, B. average time interacting with cyclones, and C. the number of cases of each interaction configuration, which is related to the number of cyclones that interact during this stagnation process.

Observing the mean interaction time (IT) in each C contour (Table 1), the longer IT is related to longer stagnation of AgRs observed in C0. This is evidenced in a stronger correlation ($r = 0.73$) between the interaction and residence times of the 117 events. Therefore, the number of cyclones does not alone guarantee a higher RT, however, it will increase the IT which, in turn, impacts the stagnation in C0.

Up to this point, it was observed that the anticyclones tend to stagnate over the C0 region, that there is a correlated simultaneous occurrence of cyclones surrounding them, and that there is a direct relationship between these factors. However, can a criterion be defined to determine whether there is a stagnation of AgRs? We have established the importance of the interaction for the stagnation process. Thus, the result from the cases where there is no interaction will enlighten us about what we can consider as a minimum RT to be considered as a stagnation period. For these cases, the mean RT is 27.7±15.4 days (∼4 weeks) (Figure 5.A, 0-bar). Thus, using 4 weeks as a threshold for stagnation, out of the 117 anticyclonic events passing through C0, only 5 are cases of non-interaction with cyclones and have RT greater than this limit. Interestingly, these non-interaction events show a merger of the southwestward propagating AgR and a stagnant one that previously had arrived in C0, justifying a longer RT, despite the absence of cyclones around. Therefore, we considered these as a pseudo-stagnation Belonenko et al. (2021) also observed pairs of eddies of opposites polarities lasting approximately for a month, considering this relationship as rather stable.

The imposition of the 4-week threshold reduces the number of cases that interact with only one cyclone (Figure S1.A). Thus, the stagnation configuration linked to the

two-cyclones interaction is the most recurrent. In this way, it is understood that as we select anticyclones that remain longer in C0, there will be a tendency to identify cases where more recurrent and lasting interactions with cyclones occur (Figure S1.B). We still must address remains how the typical configuration of this relation between opposite polarities takes place spatially.

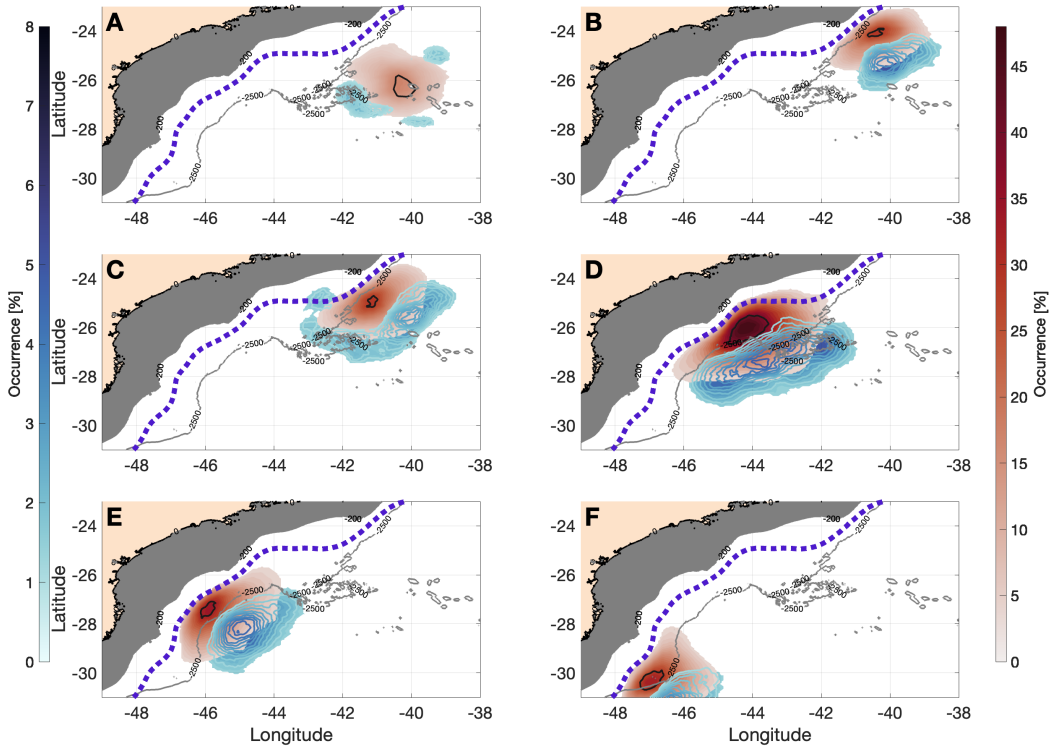

Figure 6. Occurrence rate of AgRs (shades of red) crossing the contours of the reference A. CΨ, B. C-2, C. C-1, D. C0, E. C+1, and F. C+2, and of cyclones (shades of blue) that interact with these anticyclones, between January 1993 and May 2017, based on the identification data from Laxenaire et al. (2018). In gray, the isobath of 200 and 2500 meters. In blue, the mean contour of zero-Ψ is based on values of Figure 1, representing the axis of the Brazil Current.

As previously observed, the longer persistence of AgRs in the SBB is related to a greater co-occurrence of and more lasting interaction with cyclones (Table 1). Yet, going beyond the statistical evaluation, Figure 2.B shows that there are preferred regions for the occurrence of cyclones and, consequently, for the interactivity among the eddies with opposite polarity. Therefore, we should pursue the understanding of the spatial configuration of the cyclones during these interactions in the different C-contoured areas in the SBB, and how that may affect the trapping of the AgRs.

The rate of occurrence of anticyclones, the spatial distribution, and the frequency of cyclones were found (Figure 6). In the most northern contours (Figure 6.A, B and C), there are three different settings. In the CΨ, the lowest cyclonic mean occurrence rate is found (1.8±0.3%), which is consistent with the lowest values of NC (Table 1). Due to the scattering and lack of cyclonic events around the arriving AgRs, there is low interaction between eddies of opposite polarity, and the annual occupation of this region by anticyclones is the smallest among the reference contours. These results are also directly

related to the fact that the presence of the cyclones is not necessarily a physical obstacle to the westward propagation of anticyclones. On the contrary, cyclones sometimes form a dipole structure with incoming anticyclones, propagating together, as observed in the Brazil Current domain (Arruda et al., 2013; Arruda & da Silveira, 2019), and between SBB cyclones and AgRs (Guerra et al., 2018).

One of the highest cyclonic rates is in C-2 (5.8%), where there is a concentration of episodes to the southeast of the anticyclones. In Figure 6.B, there is a pattern that repeats itself along the passage of the rings in the SBB: the AgRs not only interact with the cyclones but are constrained between them and the Brazil Current (blue contour in Figure 6). In Figures 6.B to F, the AgRs are pressed between cyclones and the BC. This is an important result because as there is an increase in anticyclonic permanence, there will be a crucial enhancement in the eddy-current interaction. That is pronounced especially at C0, where there is the highest RT, NC, and IT values. These encounters may promote changes in the exchanges between these AgRs and the mean BC structure, affecting the current speed (Guerra et al., 2018) and meandering (Soutelino et al., 2011; Rocha & Simoes-Sousa, 2022). The influence of eddies over currents was also observed in other basins (Clément et al., 2016; Shi & Wang, 2021).

In C-1, despite the increase in NC compared to C-2, there is a reduction in the maximum occurrence rate (4.5%). These differences are due to the change in the position of the cyclones relative to what we observed in C-2. There is a greater spread of cyclonic structures around the AgR in C-1, and a consequent reduction of the recurrence per grid point. In addition to the cyclones observed offshore of the anticyclones, there is interaction with cyclones from the BC, onshore: the CFE. Both inshore and offshore position cyclones, circling the anticyclones to the most southwesterly portion, with values that do not exceed 5%. Therefore, despite appearing to be a configuration that would provide more significant conditions for the stagnation of anticyclones, the low NC dilutes the cyclones around the AgRs and mitigates this potential.

In C0, as observed so far, the highest occurrences of both anticyclones (48.4%) and cyclones (7.7%) are found. Additionally, the greatest overlap of cyclonic and anticyclonic rate contours is observed at this position (Figure 6.D). This intersection is equivalent to more than 1/3 of the area occupied by anticyclones events. This information corroborates the fact that in almost 90% of the cases where an anticyclone stagnates in C0, there is at least one cyclone co-occurring.

In addition to these observations, we evaluated the AgR proximity to the BC. To do so, we use the mean contour of zero-Ψ (blue dashed line in Figure 6) as reference. This represents the center position of the BC jet core (Rocha & Simoes-Sousa, 2022). The stagnant anticyclones in C0 present one of the smallest distances to the reference among all the C areas (14.4±22.2 km) and the largest number of events where AgRs merge with the contour of the BC core. It is worth mentioning that at C-2, the AgRs begin to approach this reference (27.7±25.5 km) and get closer at C-1 (22.2±26.4 km) due to the meandering of the BC, related to the change in the orientation of the continental margin.

Synthesizing all information obtained so far, there is a greater probability of anticyclones stagnating in C0 due to interaction with cyclones, being pushed towards BC, and having, finally, their passage towards the southwest strangled and hampered. This configuration generates the trapping effect, prolonging the stay of the AgRs in the region, and causes a certain eddy deformation, altering the more circular shape of the stagnant feature, to a more elongated shape. We can observe this fact in Figures 1.B and 2.B (red contour). Hence, the average radii of AgRs decrease from 121.2 km at C0 to 115.0 km at C+1.

The rings continue to be strongly influenced by offshore cyclones in C+1, where we obtained the second highest occurrence rates of anticyclones (35.7%) and cyclones (7.2%). However, despite the similar number of anticyclones in C0 and C+1 (AY in the Table 1), the number of cyclones and the interaction time are importantly reduced from 219 to 169, and from 25.2 days to 14.6 days, respectively. Therefore, the AgRs continue to be squeezed against BC, but without the same stagnation effect.

Finally, at the exit of the SBB region, we can observe the end of the crossing of the AgRs in C+2 contour. At this point, the occurrence of anticyclones (33.8%) is still higher than those observed in the contours northern of C0. However, the same high occurrence does not happen for the cyclones (5.4%). As observed so far, this low occurrence impacts the IT, which consequently, creates the condition for the AgR being more distant from the BC (27.5±27.5 km). The sum of these factors results in the lowest RT among all the C contours.

7 Summary and final remarks

The South Brazil Bight is a region populated by high vortical activity, both cyclonic and anticyclonic. Through the application of altimeter data, the signal of these mesoscale features can be observed along the bight. Among what was observed, two scenarios stand out: the eddy corridor together with the Brazil Current meandering structure, and a strong signal possibly related to an anticyclonic feature, surrounded by cyclonic features, over the São Paulo Plateau. From these observations, we initially investigated the passage of anticyclonic eddies through the region, to better understand the reason for the existence of a more intense signal over the plateau region.

To investigate the signature observed over the São Paulo Plateau, we used the eddy identification and tracking dataset developed by Laxenaire et al. (2018), from which we can extract information such as the position in time and space of the vortex core and its contour is determined. In addition, the set considers the processes of merging and splitting of vortices to establish connections between different vortical structures. This allowed us to follow both the passage of anticyclones through the region and the origin of these eddies. Aiming to evaluate the pathway of these anticyclones in the South Brazil Bight, we determined a region with a high occurrence rate of these eddies as a reference for the analyses. Which in turn coincided with the São Paulo Plateau location, where we counted over time the anticyclonic structures that crossed it.

Between January 1993 and mid-May 2017, 136 anticyclones were observed crossing the control region, of which 117 have connections that trace back their origin to the Agulhas Leakage region. Although only 3 of these are anticyclones that directly cross the South Atlantic (order 0th), a wide influence of the Agulhas Rings on the South Brazil Bight was noted. According to the Laxenaire et al. (2018) identification, most of the anticyclones that reach the South Brazil Bight are classified as higher-order eddies, since they were subjected to nonlinear interactions (successive merging and splitting). The Agulhas Rings that cross the control contour, approach the South Brazil Bight in the latitudinal range from 24° S to 26° S, without a preferred latitude or route.

Jointly with the arrival of the Agulhas Rings at the South Brazil Bight, we observe the co-occurrence of cyclones interacting with the anticyclones. What we can observe is that these cyclones have varied origins. In addition to the well-documented presence of locally formed cyclones from the Brazil Current meanders, we observed that most of the cyclones that interact with the anticyclones had a remote formation. As the Agulhas Rings approach the westernmost portion of the South Atlantic, the contact with the cyclone increases, both in terms of recurrence and duration of these interactions. With the occurrence of this relationship between eddies of opposite polarity, the anticyclones, when approaching the coastal region, begin to also interact with the Brazil Current.

Not only do these Agulhas Rings arrive and cross the basin region, but they also show a marked permanence (50.8±31.8 days) in the control contour, with an average occurrence of 5.3±1.3 anticyclones per year. Compared to other regions within South Brazil Bight, this permanence is almost 60% longer, despite the occurrence per year, on average, not being higher in the same proportion. This showed us that the signal observed in the altimeter data is more related to a longer permanence of these anticyclones than to a greater recurrence of these features of such polarity over the plateau region.

When observing the occurrence of cyclones around the anticyclonic events, what caught our attention was that in the São Paulo Plateau region, the largest number of cyclone-anticyclone interactions occur (219), for the longest time (25.2±22.8 days). Due to this higher recurrence and duration, these interactions generate a shielding process, where an anticyclone is surrounded by at least one eddy of opposite polarity and has its translation impacted, being restrained, blocked, or redirected. In the unprecedented case of the present study, these shielded anticyclones are even more squeezed by these cyclones towards the Brazil Current, as soon as they begin to approach the 2500-meter isobath. Under this stagnation process over the control contour, we observed that Agulhas Rings can meld with the anticyclonic lobe of the Brazil Current. Because of the shielding phenomenon, the Agulhas Rings maintain their integrity, and splitting is absent. This is due to the assessment that shielded eddies tend to be stable (Reinaud, 2017). By observing the effect on the permanence of anticyclones over the São Paulo Plateau, we conclude that the interaction time is the substantial factor for the longer permanence of these anticyclones. As consequence, important eddy-eddy and eddy-current interactions are promoted, allowing property exchanges between these regionally dominant structures.

The end of stagnation occurs with the mitigation of the shielding process. This change is directly related to the reduction in the occurrence of cyclones and the change in the spatial distribution of these features around the anticyclones. As consequence, there is a movement away from the Brazil Current. The anticyclones that maintain their integrity, will head southwestward until they leave the South Brazil Bight. Although the cyclone-anticyclone-Brazil Current interactions in this southern limb of the bight do not provide the same pattern of stagnation of the anticyclones in the control region, the Agulhas Rings remain over the 2500-m isobath.

In conclusion, the entire passage of anticyclones, mostly connected to the Agulhas Leakage, is influenced by several interactions with local and remote cyclones and the Brazil Current. As these anticyclones cross the SBB, both the interaction with cyclones and the translation time of Agulhas Rings tend to increase as they approach the São Paulo Plateau region. The peak of the residence time is reached in the control contour because of the shielding process. The impact of this longer stay in a specific region of the South Brazil Bight, linked to greater interaction with cyclones and the Brazil Current, is an unexplored and an important topic for the studies of eddy dynamics along the western boundary currents. The fate of the Agulhas Ring as they approach the Brazil Current retroflection region is yet to be unraveled.

Acknowledgments

The SSALTO/DUACS altimeter products were produced and distributed by the Copernicus Marine and Environment Monitoring Service (CMEMS) (http://www.marine.copernicus.eu). The Argo data were collected and made freely available by the International Argo Program and the national programs that contribute to it. (https://argo.ucsd.edu, https://www.ocean-ops.org). The Argo Program is part of the Global Ocean Observing System (https://doi.org/10.17882/42182). We also would like to thank PETROBRAS for their partnership in regard the Project Santos. I.C.A.S., P.S.B. and C.Z.L. acknowledges support from CNPq (Project HIDROSAN I, 405593/2021-0) and FAPESP (Project HIDROSAN II, 2021/13124-6).

References

Arruda, W. Z., Campos, E. J., Zharkov, V., Soutelino, R. G., & da Silveira, I. C. (2013). Events of equatorward translation of the Vitoria Eddy. *Continental Shelf Research*, *70*, 61–73.

Arruda, W. Z., & da Silveira, I. C. (2019). Dipole-induced central water extrusions south of Abrolhos Bank (Brazil, 20.5 oS). *Continental Shelf Research*, *188*, 103976.

Assireu, A., Stevenson, M., & Stech, J. (2003). Surface circulation and kinetic energy in the SW Atlantic obtained by drifters. *Continental Shelf Research*, *23*(2), 145–157.

Azevedo, J. L., Nof, D., & Mata, M. M. (2012). Eddy-train encounters with a continental boundary: A South Atlantic case study. *Journal of physical oceanography*, *42*(9), 1548–1565.

Beal, L. M., De Ruijter, W. P., Biastoch, A., & Zahn, R. (2011). On the role of the Agulhas system in ocean circulation and climate. *Nature*, *472*(7344), 429–436.

Belo, W. C. (2011). A Recirculação Interna do Giro Subtropical do Atlântico Sul e a Circulação Oceânica na Região do Pólo Pré-sal da Bacia de Santos. *Diss. Universidade de São Paulo*.

Belonenko, T., Zinchenko, V., Fedorov, A., Budyansky, M., Prants, S., & Uleysky, M. Y. (2021). Interaction of the Lofoten vortex with a satellite cyclone. *Pure and Applied Geophysics*, *178*(1), 287–300.

Biastoch, A., Böning, C. W., Schwarzkopf, F. U., & Lutjeharms, J. R. E. (2009). Increase in Agulhas leakage due to poleward shift of Southern Hemisphere westerlies. *Nature*, *462*(7272), 495–498.

Böebel, O., Davis, R. E., Ollitraut, M., Peterson, R. G., Richard, P. L., Schmid, C., & Zenk, W. (1999,). The intermediate depth circulation of the Western South Atlantic. *Geophysical Research Letters*, *26*(21), 3329–3332.

Calado, L., Gangopadhyay, A., & Da Silveira, I. (2006). A parametric model for the Brazil Current meanders and eddies off southeastern Brazil. *Geophysical Research Letters*, *33*(12).

Calado, L., Gangopadhyay, A., & Da Silveira, I. (2008). Feature-oriented regional modeling and simulations (FORMS) for the western South Atlantic: Southeastern Brazil region. *Ocean Modelling*, *25*(1-2), 48–64.

Calado, L., Silveira, I. C. A. d., Gangopadhyay, A., & Castro, B. M. (2010). Eddy–induced upwelling off Cape São Tomé (22°S, Brazil). *Continental Shelf Research*, *30*(10–11), 1181–1188.

Campos, E. J. D., Velhote, D., & Silveira, I. C. A. d. (2000). Shelf break upwelling driven by Brazil Current cyclonic meanders. *Geophysical Research Letters*, *27*(6), 751–754.

Capuano, T. A., Speich, S., Carton, X., & Laxenaire, R. (2018). Indo-Atlantic Exchange, Mesoscale Dynamics, and Antarctic Intermediate Water. *Journal of Geophysical Research: Oceans*, *123*(5), 3286–3306.

Carton, X. (1992). On the merger of shielded vortices. *EPL (Europhysics Letters)*, *18*(8), 697.

Carton, X. (2001). Hydrodynamical modeling of oceanic vortices. *Surveys in Geophysics*, *22*(3), 179–263.

Castro, B. d., & Miranda, L. d. (1998). Physical oceanography of the western Atlantic continental shelf located between 4°N and 34°S. *The sea*, *11*(1), 209–251.

Clément, L., Frajka-Williams, E., Sheen, K., Brearley, J., & Garabato, A. N. (2016). Generation of internal waves by eddies impinging on the western boundary of the North Atlantic. *Journal of Physical Oceanography*, *46*(4), 1067–1079.

Cushman-Roisin, B., Tang, B., & Chassignet, E. P. (1990). Westward motion of mesoscale eddies. *Journal of Physical Oceanography*, *20*(5), 758–768.

de Ruijter, W. d., Biastoch, A., Drijfhout, S., Lutjeharms, J., Matano, R., Pichevin, T., ... Weijer, W. (1999). Indian-Atlantic interocean exchange: Dynamics, estimation and impact. *Journal of Geophysical Research: Oceans*, *104*(C9), 20885–20910.

Escudier, R., Renault, L., Pascual, A., Brasseur, P., Chelton, D., & Beuvier, J. (2016). Eddy properties in the Western Mediterranean Sea from satellite altimetry and a numerical simulation. *Journal of Geophysical Research: Oceans*, *121*(6), 3990–4006.

Garzoli, S., & Gordon, A. (1996). Origins and variability of the Benguela Current. *Journal of Geophysical Research: Oceans*, *101*(C1), 897–906.

Gordeeva, S., Zinchenko, V., Koldunov, A., Raj, R. P., & Belonenko, T. (2021). Statistical analysis of long-lived mesoscale eddies in the Lofoten Basin from satellite altimetry. *Advances in Space Research*, *68*(2), 364–377.

Gordon, A. L. (1986). Interocean exchange of thermocline water. *Journal of Geophysical Research: Oceans*, *91*(C4), 5037–5046.

Gordon, A. L., Weiss, R. F., Smethie, W. M., & Warner, M. J. (1992). Thermocline and intermediate water communication between the South Atlantic and Indian oceans. *Journal of Geophysical Research*, *97*(C5), 7223. doi: {10.1029/92jc00485}

Guerra, L. A. A., Mill, G. N., & Paiva, A. M. (2022). Observing the spread of Agulhas Leakage into the Western South Atlantic by tracking mode waters within ocean rings. *Frontiers in Marine Science*, *9*, 958733.

Guerra, L. A. A., Paiva, A. M., & Chassignet, E. P. (2018). On the translation of Agulhas rings to the western South Atlantic Ocean. *Deep Sea Research Part I: Oceanographic Research Papers*, *139*, 104–113.

Kennelly, M. A., Evans, R. H., & Joyce, T. M. (1985). Small-scale cyclones on the periphery of a Gulf Stream warm-core ring. *Journal of Geophysical Research: Oceans*, *90*(C5), 8845–8857.

Laxenaire, R., Speich, S., Blanke, B., Chaigneau, A., Pegliasco, C., & Stegner, A. (2018). Anticyclonic eddies connecting the western boundaries of Indian and Atlantic Oceans. *Journal of Geophysical Research: Oceans*, *123*(11), 7651–7677.

Laxenaire, R., Speich, S., & Stegner, A. (2020). Agulhas Ring Heat Content and Transport in the South Atlantic Estimated by Combining Satellite Altimetry and Argo Profiling Floats Data. *Journal of Geophysical Research: Oceans*, *125*(9), e2019JC015511.

Lazaneo, C. Z., Napolitano, D. C., da Silveira, I. C., Tandon, A., MacDonald, D. G., Ávila, R. A., & Calil, P. H. (2020). On the role of turbulent mixing produced by vertical shear between the Brazil Current and the Intermediate Western Boundary Current. *Journal of Geophysical Research: Oceans*, *125*(1), e2019JC015338.

Lutjeharms, J., & Cooper, J. (1996). Interbasin leakage through Agulhas Current filaments. *Deep Sea Research Part I: Oceanographic Research Papers*, *43*(2), 213–238.

Lutjeharms, J., & Gordon, A. (1987). Shedding of an Agulhas ring observed at sea. *Nature*, *325*(6100), 138–140.

Lutjeharms, J., & Van Ballegooyen, R. (1988). The retroflection of the Agulhas Current. *Journal of Physical Oceanography*, *18*(11), 1570–1583.

Mano, M. F., Paiva, A. M., Torres Jr, A. R., & Coutinho, A. L. (2009). Energy flux to a cyclonic eddy off Cabo Frio, Brazil. *Journal of Physical Oceanography*, *39*(11), 2999–3010.

Mill, G. N., da Costa, V. S., Lima, N. D., Gabioux, M., Guerra, L. A. A., & Paiva, A. M. (2015). Northward migration of Cape São Tomé rings, Brazil. *Continental Shelf Research*, *106*, 27–37.

Napolitano, D. C., Rocha, C. B., da Silveira, I. C., Simoes-Sousa, I. T., & Flierl,

760 G. R. (2021). Can the Intermediate Western Boundary Current recirculation
761 trigger the Vitória Eddy formation? *Ocean Dynamics*, *71*(3), 281–292.
762 Nencioli, F., Dall'Olmo, G., & Quartly, G. D. (2018). Agulhas Ring Transport
763 Efficiency From Combined Satellite Altimetry and Argo Profiles. *Journal of*
764 *Geophysical Research: Oceans*, *123*(8), 5874-5888. Retrieved from {https://
765 agupubs.onlinelibrary.wiley.com/doi/abs/10.1029/2018JC013909} doi:
766 {https://doi.org/10.1029/2018JC013909}
767 Ni, Q., Zhai, X., Wang, G., & Hughes, C. W. (2020). Widespread mesoscale dipoles
768 in the global ocean. *Journal of Geophysical Research: Oceans*, *125*(10),
769 e2020JC016479.
770 Oliveira, L. R., Piola, A. R., Mata, M. M., & Soares, I. D. (2009). Brazil Current
771 surface circulation and energetics observed from drifting buoys. *Journal of*
772 *Geophysical Research: Oceans*, *114*(C10).
773 Olson, D. B., & Evans, R. H. (1986). Rings of the Agulhas current. *Deep Sea Re-*
774 *search Part A. Oceanographic Research Papers*, *33*(1), 27–42.
775 Palóczy, A., Silveira, I. d., Castro, B., & Calado, L. (2014). Coastal upwelling off
776 Cape São Tomé (22 S, Brazil): The supporting role of deep ocean processes.
777 *Continental Shelf Research*, *89*, 38–50.
778 Pereira, F., da Silveira, I. C., Flierl, G. R., & Tandon, A. (2019). NPZ response to
779 eddy-induced upwelling in a Brazil Current ring: A theoretical approach. *Dy-*
780 *namics of Atmospheres and Oceans*, *87*, 101096.
781 Prants, S. (2015). Backward-in-time methods to simulate large-scale transport and
782 mixing in the ocean. *Physica Scripta*, *90*(7), 074054.
783 Prants, S., Budyansky, M., Lobanov, V., Sergeev, A., & Uleysky, M. Y. (2020).
784 Observation and Lagrangian Analysis of Quasi-Stationary Kamchatka Trench
785 Eddies. *Journal of Geophysical Research: Oceans*, *125*(6), e2020JC016187.
786 Prants, S., Budyansky, M., & Uleysky, M. Y. (2018). How eddies gain, retain, and
787 release water: A case study of a Hokkaido anticyclone. *Journal of Geophysical*
788 *Research: Oceans*, *123*(3), 2081–2096.
789 Pujol, M., & Mertz, F. (2019). Product user manual for sea level SLA products.
790 *Copernicus Marine Monitoring Service.*.
791 Reinaud, J. N. (2017). Piecewise uniform potential vorticity pancake shielded vor-
792 tices. *Geophysical & Astrophysical Fluid Dynamics*, *111*(1), 32–64.
793 Renault, L., Marchesiello, P., Masson, S., & Mcwilliams, J. C. (2019). Remarkable
794 control of western boundary currents by eddy killing, a mechanical air-sea
795 coupling process. *Geophysical Research Letters*, *46*(5), 2743–2751.
796 Rocha, C. B., Silveira, I. C. A. d., Castro, B. M., & Lima, J. A. M. (2014). Vertical
797 structure, energetics, and dynamics of the Brazil Current System at 22°S–28°S.
798 *Jounal Geophysical Research*, *119*(1), 52–69. Retrieved from {http://
799 dx.doi.org/10.1002/2013JC009143} doi: {10.1002/2013JC009143}
800 Rocha, C. B., & Simoes-Sousa, I. T. (2022). Compact Mesoscale Eddies in the South
801 Brazil Bight. *Remote Sensing*, *14*(22), 5781.
802 Schmid, C., Schäfer, H., Zenk, W., & Podestá, G. (1995). The Vitória eddy and its
803 relation to the Brazil Current. *Journal of physical oceanography*, *25*(11), 2532–
804 2546.
805 Schouten, M. W., de Ruijter, W. P., Van Leeuwen, P. J., & Lutjeharms, J. R.
806 (2000). Translation, decay and splitting of Agulhas rings in the southeast-
807 ern Atlantic Ocean. *Journal of Geophysical Research: Oceans*, *105*(C9),
808 21913–21925.
809 Shi, Q., & Wang, G. (2021). Meander Response of the Kuroshio in the East China
810 Sea to Impinging Eddies. *Journal of Geophysical Research: Oceans*, *126*(9),
811 e2021JC017512.
812 Silveira, I. C. A. d., Calado, L., Castro, B., Cirano, M., Lima, J., & Mascarenhas,
813 A. d. S. (2004). On the baroclinic structure of the Brazil Current–Intermediate
814 Western Boundary Current system at 22–23 S. *Geophysical research letters*,

31(14).

Silveira, I. C. A. d., Lima, J. A. M., Schmidt, A. C. K., Ceccopieri, W., Sartori, A., Franscisco, C. P. F., & Fontes, R. F. C. (2008). Is the meander growth in the Brazil Current system off Southeast Brazil due to baroclinic instability? *Dynamics of Atmospheres and Oceans*, *45*(3), 187–207.

Silveira, I. C. A. d., Pereira, F., Flierl, G. R., Simoes-Sousa, I. T., Palóczy, A., Borges-Silva, M., & Rocha, C. B. (2023). The Brazil Current quasi-stationary unstable meanders at 22° S–23° S. *Progress in Oceanography*, *210*, 102925.

Silveira, I. C. A. d., Schmidt, A. C. K., Campos, E. J. D., Godoi, S. S. d., & Ikeda, Y. (2000). A corrente do Brasil ao largo da costa leste brasileira. *Revista Brasileira de Oceanografia*, *48*, 171–183.

Soutelino, R., Da Silveira, I., Gangopadhyay, A., & Miranda, J. (2011). Is the Brazil Current eddy-dominated to the north of 20 S? *Geophysical Research Letters*, *38*(3).

Soutelino, R., Gangopadhyay, A., & Da Silveira, I. (2013). The roles of vertical shear and topography on the eddy formation near the site of origin of the Brazil Current. *Continental Shelf Research*, *70*, 46–60.

Souza, J., Chapron, B., & Autret, E. (2014). The surface thermal signature and air–sea coupling over the Agulhas rings propagating in the South Atlantic Ocean interior. *Ocean Science*, *10*(4), 633–644.

Uchoa, I., Simoes-Sousa, I. T., & da Silveira, I. C. (2022). The Brazil Current mesoscale eddies: Altimetry-based characterization and tracking. *Deep Sea Research Part I: Oceanographic Research Papers*, 103947.

Zembruscki, S. (1979). Geomorfologia da margem continental sul brasileira e das bacias oceânicas adjacentes. In *PROJETO REMAC: geomorfologia da margem continental brasileira e das áreas oceânicas adjacentes* (p. 129-177). Rio de Janeiro: PETROBRAS. CENPES. DINTEP (Série REMAC no. 7).

Figure 1.

A

B

Latitude

Longitude

Cape Frio

Cape Santa Marta

São Paulo Plateau

Ψ [$m^2 s^{-1}$]

$\times 10^{-3}$

Figure 2.

A

B

Latitude

Longitude

-23
-24
-25
-26
-27
-28
-29
-30
-31

-49
-48
-47
-46
-45
-44
-43
-42
-41
-40
-39
-38

C0
CΨ
C-2
C-1
C+1
C+2

Occurrence [%]

35
30
25
20
15
10
5
0

25
20
15
10
5
0

Figure 3.

A

B

Latitude

Longitude

Distance [km]

N° of eddies

Figure 4.

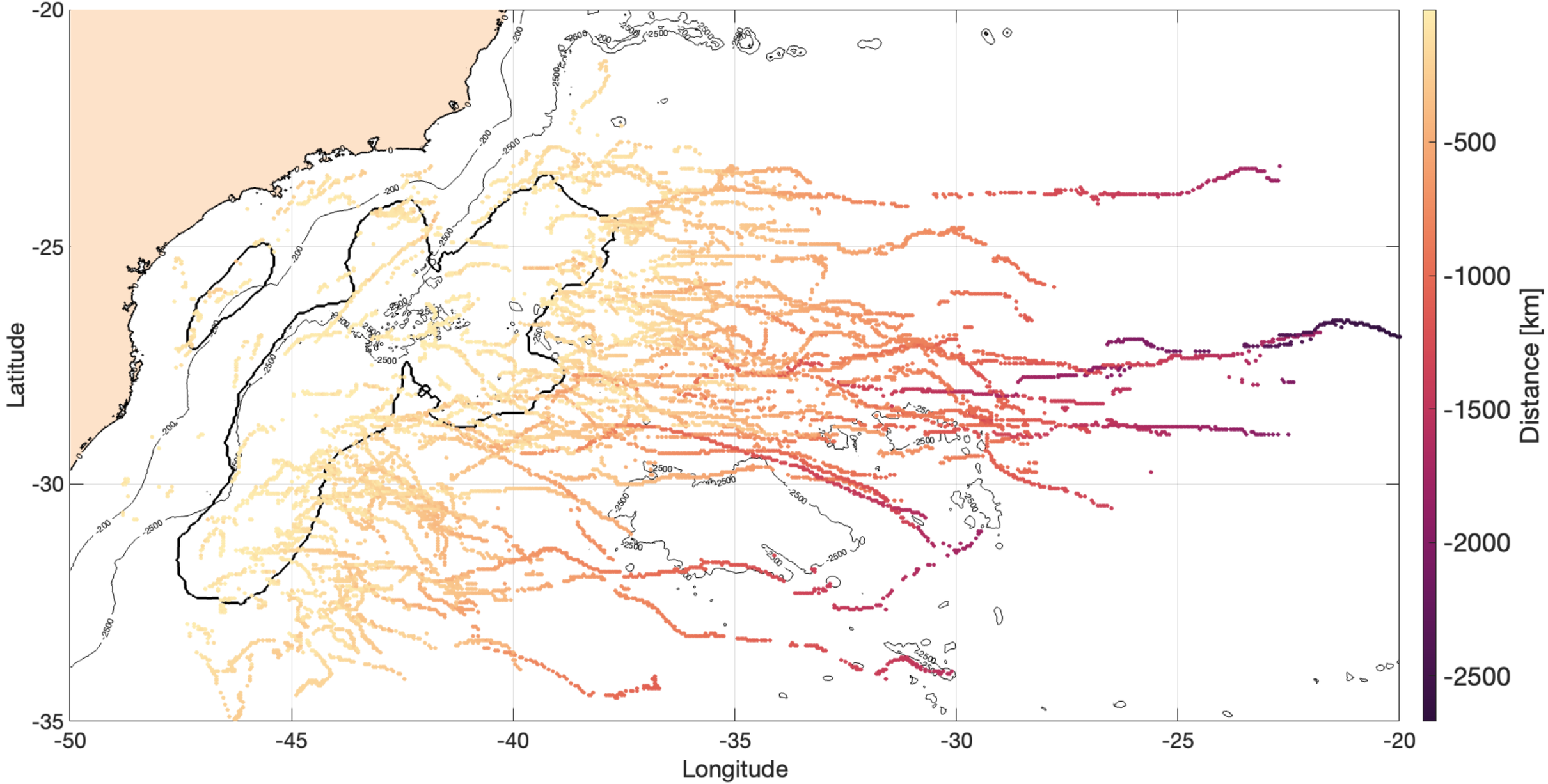
-20
-25
-30
-35
Latitude
-50
-45
-40
-35
-30
-25
-20
Longitude
-500
-1000
-1500
-2000
-2500
Distance [km]

Figure 5.

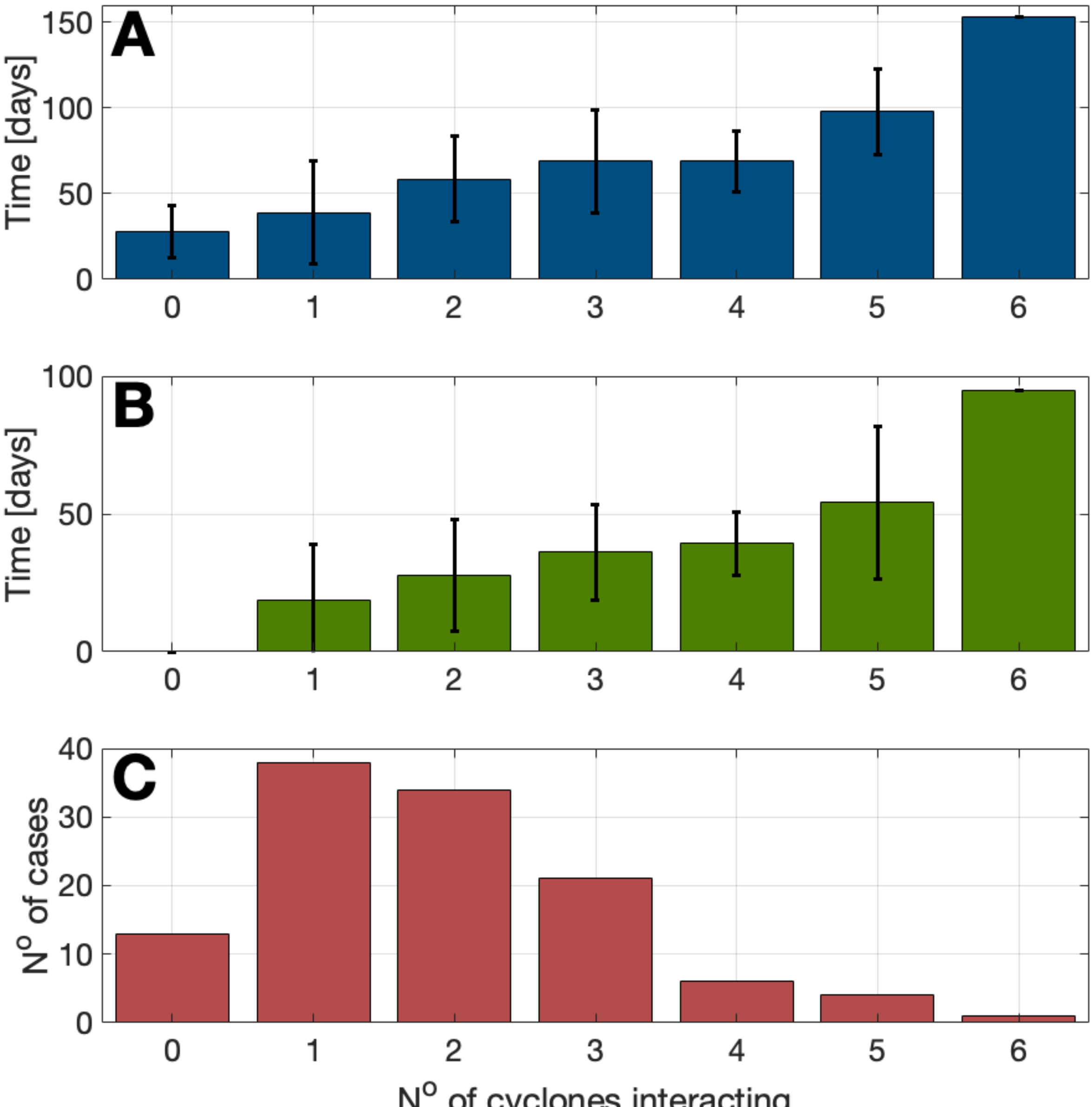
A
Time [days]
150
100
50
0
0
1
2
3
4
5
6
B
Time [days]
100
50
0
0
1
2
3
4
5
6
C
N° of cases
40
30
20
10
0
0
1
2
3
4
5
6
N° of cyclones interacting

Figure 6.

A
B
C
D
E
F
Latitude
Longitude
-24
-26
-28
-30
-48
-46
-44
-42
-40
-38
0
-200
-2500
Occurrence [%]
8
7
6
5
4
3
2
1
0
45
40
35
30
25
20
15
10
5
0